Indian Journal of Chemical Technology
Vol. 28, July 2021, pp. 421-428

Effect of 1,2,3- triazole derivative on the dissolution performance of mild steel in 1M HCl medium

K Vijayalakshmi, N Punitha, R Rengamy & J Elangovan*

PG and Research Department of Chemistry, Rajah Serfoji Government College (Autonomous), Thanjavur 613 005, Tamilnadu, India.

(Affiliated to Bharathidasan University, Thiruchirappalli 620 024, Tamilnadu, India.)

E-mail: elangoorganic@gmail.com

Received 31 August 2020; accepted 17 June 2021

The corrosion mitigation behaviour of 1-benzyl-4-(naphthalen-2-yl)-1*H*-1,2,3-triazole (BNT) has been explored on mild steel in 1M HCl medium employing chemical and electrochemical techniques. The observed results illustrate that the hindered efficacy was increased as increasing concentration of BNT and with rising temperatures. The electrochemical studies point out that the inspected BNT is a mixed kind inhibitor and the adsorption isotherm discussions proposed the inhibition mechanism obeyed Langmuir isotherm. The kinetic and thermodynamical parameters exposed that the adsorption process is endothermic, spontaneous and the mechanism is both physical and chemical adsorption. Further, the morphological investigations have been carried out by SEM, EDS and AFM techniques. The highest efficiency perceived for BNT is found to be 91.35% and behaved as a proficient inhibitor against mild steel corrosion in the 1M HCl environment.

Keywords: Corrosion, Electrochemical, Kinetic, Langmuir isotherm, Triazole.

Mild steels are one of the most essential materials employed in human desires and they discover many applications, especially for construction, automobiles and industrial works[1,2]. Even though mild steels encompassing a wide range of applications, they are sternly pretentious by corrosion when they are in contact with acidic atmosphere and other chemical processes[3,4].

Meanwhile, the environmental hazards also influenced the quality of mild steels and the rusting of mild steels more easily occur in the acidic and humid atmosphere[5]. The corrosion concert of mild steel and its alloys are primarily dependent on their composition and microstructure[6]. Also, environmental factors such as temperature and degree of aeration are affected by this corrosion recital. Hence, corrosion is one of the noteworthy and costliest harms around the globe. In previous decades, many endeavors have been put into practice to resolve these problems and utilization of inhibitors is the universally accepted and widely utilized technique for curtailing the rate of corrosion. In this circumstance, organic inhibitors are employed as the foremost anti-corrosion candidates comprising heteroatoms such as nitrogen, oxygen and sulphur for mild steels in assorted corrosive environments[7-12].

In recent years, 1,2,3- triazoles derivatives have great attention to employing the mitigation of corrosion rate in different aggressive media[13-15]. Moreover, the hindered efficiency chiefly depends on their molecular structure, presence of heteroatoms, substituent effect, π electron density and petite toxicity of the triazole derivatives[16-18].

In this study, 1-benzyl-4-(naphthalen-2-yl)-1H-1,2,3-triazole (BNT) was used to evaluate the corrosion inhibition performance on mild steel in 1M HCl medium and the molecular structure of BNT is given in Fig. 1.

Experimental Section

Materials

Mild steel specimens (IRS M41/97steel) utilized in the present investigation comprising the elemental composition (wt %) were P- 0.089, Si- 0.319, Mn-0.43%, S-0.009, Al-0.028, C-0.076, Cr-0.52, Ni- 0.20, Cu-0.31 and Fe-99.69. For the mass loss method, the rectangular-shaped mild steel specimens enclosing the dimensions 5cm × 2cm × 0.2cm were employed. Mild steel specimens were prepared by different numbers (up to 1500) of SiC emery papers and the polished specimens were washed with distilled water, rinsed with ethanol and degreased with acetone[19].

A corrosive solution (1M HCl) was prepared for the gravimetric experiments from 37% Analar HCl

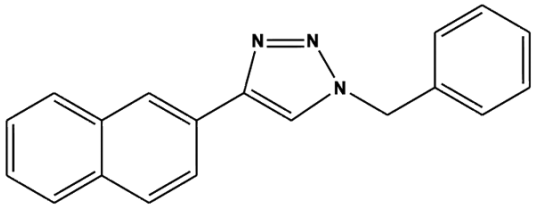

Fig.1 — 1-benzyl-4-(naphthalen-2-yl)-1*H*-1,2,3-triazole (BNT)

with distilled water. Meanwhile, BNT was synthesized and characterized by melting point, FT-IR, ^{1}H NMR and ^{13}C NMR analysis[20]. The desired concentrations of BNT were prepared in ethanol for further measurements.

Gravimetric method

The gravimetric analysis was performed using accurately weighed polished mild steel specimens before and after immersion in 1M HCl solution with 10, 30, 50 and 100 ppm concentrations of BNT for six hours exposure time at room temperature. Further, all the experiments were carried out in thrice for the determination of mean mass loss values with the same conditions. From the average mass loss, the corrosion factors such as corrosion rate, inhibition efficiency and surface coverage were calculated by equations 1, 2 and 3 respectively..

$$CR = \frac{\Delta W}{At} \qquad ...(1)$$

where ΔW is the mean mass loss (mg), A is the total area (cm^{-2}) and t is the immersion time (h) in the presence and absence of BNT in 1M HCl solution.

$$I.E(\%) = \left(\frac{W_o - W}{W_o} \right) \times 100 \qquad ...(2)$$

$$\theta = \left(\frac{W_o - W}{W_o} \right) \qquad ...(3)$$

where W_o and W are the mean mass loss (mg) of mild steels in the absence and presence of BNT in 1M HCl solution respectively.

Electrochemical techniques

Polarization measurements

The potentiodynamic polarization assessments were executed by a three-electrode CH instrument (CHI-66 model). Herein, a platinum foil was used as a counter electrode and a standard calomel electrode was employed as a reference electrode. Besides, $1cm^{-2}$ area of the test specimen was immersed in 1M HCl in the presence and absence of the BNT performed as a working electrode and this area of the test specimens was fixed throughout the experiments. Before every measurement, the stabilization period 30 min was applied to attain the open circuit potential. After that, the polarization curves were acquired by varying the electrode potential from -500 mV to +500 mV.

From the Tafel extrapolation technique, the corrosion current density (I_{corr}) values were obtained and inhibition efficiencies for all the working concentrations were calculated using equation 4

$$IE(\%) = \left[\frac{i_{corr} - i_{corr}(inh)}{i\,corr} \right] \times 100 \qquad ...(4)$$

where $I_{corr\ (inh)}$ and I_{corr} are the corrosion current densities in the presence and absence of BNT in 1M HCl solution.

Impedance study

The electrochemical impedance study was conducted with CH instrument and the impedance parameters were acquired from the Nyquist plots in the frequency range between 100 kHz and 10 MHz. Charge Transfer Resistance (R_{ct}) and electrical double layer capacity (C_{dl}) was achieved from the Nyquist plots. The inhibition efficiency (IE %) and electrical double layer capacity (C_{dl}) values were determined from the charge transfer resistance values using equations 5 and 6 respectively.

$$I.E(\%) = \left[\frac{R_{ct}(inh) - R_{ct}}{R_{ct}(inh)} \right] \times 100 \qquad ...(5)$$

$$CdI = \frac{1}{2\pi\pi_{max}.RC_{ct}} \qquad ...(6)$$

where and $R_{ct(inh)}$ and R_{ct} are the charge transfer resistance in the presence and absence of BNT in 1M HCl solution and f_{max} is the highest peak frequency of the Nyquist plots.

Surface morphology

The morphological examinations of the tested mild steel specimens were conducted by Scanning Electron microscope (SEM), Electron dispersive spectrum (EDS), and Atomic Force Microscope (AFM) techniques. For this exploration, the mild steel specimens were immersed in 1M HCl in the absence

and optimum concentration of BNT for 6 hours of exposure time.

Results and Discussion

Mass loss study

Figure 2 shows the correlation between the corrosion rates and inhibition efficiencies of various concentrations of BNT in the 1M HCl solution. As shown in Fig. 2 and Table 1, inhibition efficiencies increase with increasing concentration of BNT and the corrosion rates decrease correspondingly[21]. Inspection of Table 1 also reveals the maximum efficacy is 91.35% at 100 ppm. Meanwhile, the increasing values of surface coverage suggesting BNT species protect the large area of the metal with increasing concentration. These observations showed that the corrosion rates for mild steels are mitigated by the adsorption of BNT species in an acidic environment.

Electrochemical techniques

Polarization study

Tafel polarization curves for different concentrations of BNT in 1M HCl solution are shown in Fig. 3 and the electrochemical polarization parameters are presented in Table 2. As we can see from Fig 3 and Table 2, the values of corrosion potential (E_0) in the presence inhibitor are less than ± 85 mV with respect to the blank solution which indicates BNT acts as a mixed type inhibitor[22]. It also evident from the values of Tafel slopes that the polarization occurs on both sides but cathodic polarization is more predominant than the anodic move. Besides that, the values of corrosion current density (I_0) decrease with increasing concentration of BNT which exposes the electrochemical corrosion reactions are hindered by the adsorption of BNT on mild steel specimens. Also, the optimum efficiency observed is 90.12% at 100 ppm. All the polarization findings conclude that BNT performed as a potential protector in the 1M HCl medium.

Impedance study

Figure 4 exhibits the Nyquist plots of different concentrations of BNT in 1M HCl solution and the diameter of the loops increases with increasing concentration of BNT which suggests that the hindrance of charge transfer in the presence of BNT. It also explains the obtained plots are not perfect circles due to the roughness of the metallic surface and uneven distribution of active centers during the corrosion process[23]. Table 2 shows the decreasing values C_{dl} with increasing concentration of BNT which designates the increasing thickness of the electrical double layer at metal solution interface prevents the metallic surface from rust formation in 1M HCl solution. Further, the highest efficiency attained in this study is 90.60% which corroborates

Table 1 — Effect of BNT concentration on mild steel corrosion in 1M HCl

Conc. (ppm)	Corrosion rate ($mg.cm^{-2}.h^{-1}$)	Inhibition efficiency (IE %)	Surface coverage (θ)
Blank	0.4894	-	-
10	0.3238	33.83	0.34
30	0.1022	79.12	0.79
50	0.0695	85.79	0.86
100	0.0423	91.35	0.91

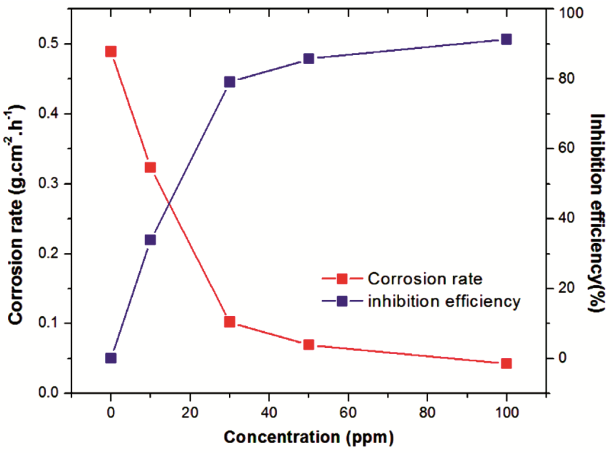

Fig. 2 — Correlation between the corrosion rates and inhibition efficiencies for BNT on mild steel specimens in 1M HCl

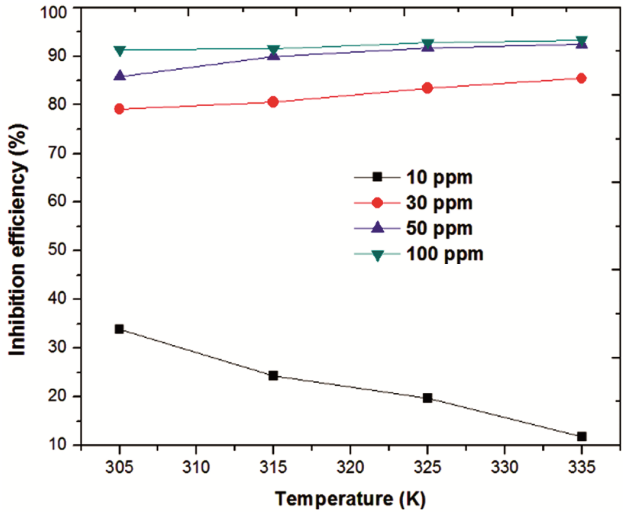

Fig. 3 — Effect of temperature on inhibition efficiencies for various concentrations of BNT on mild steel specimens in 1M HCl

Table 2 — Electrochemical polarization and impedance parameters for BNT on mild steel specimens in 1M HCl

Conc.(ppm)	Polarization parameters					Impedance parameters		
	E_0 (mV)	I_0 (mA)	b_c (mV)	b_a(mV)	IE (%)	R_{ct} ($\Omega.cm^2$)	C_{dl} ($\mu F.cm^{-2}$)	IE (%)
Blank	-420.613	3.46	995.82	254.55	0	9.45	3.2095	0
10	-487.864	2.05	97.82	262.02	40.90	16.61	1.2369	43.11
30	-449.694	0.63	672.88	561.31	81.68	49.26	0.1626	80.82
50	-437.671	0.56	153.55	102.96	83.96	81.77	0.0513	88.44
100	-436.141	0.34	161.80	78.76	90.12	100.55	0.0241	90.60

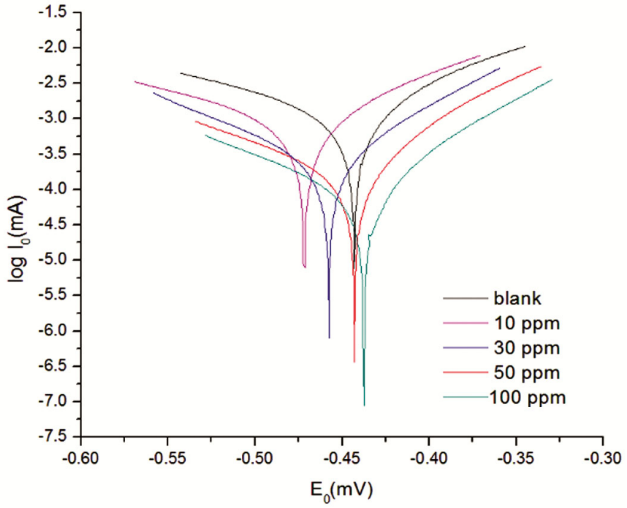

Fig. 4 — Tafel polarization curves for various concentrations of BNT on mild steel samples in 1M HCl

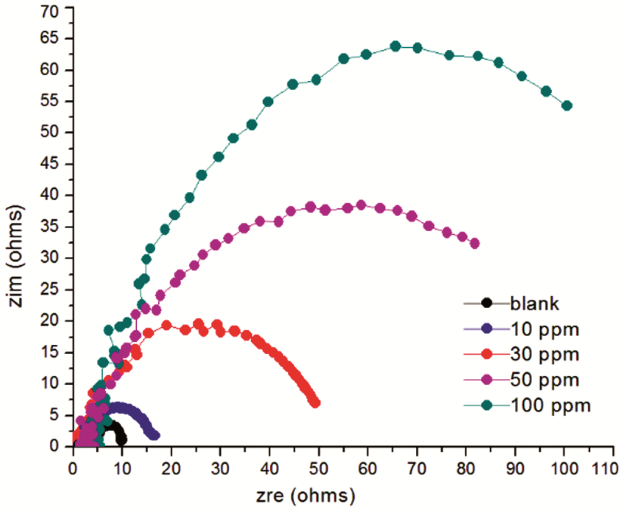

Fig. 5 — Nyquist plots for various concentrations of BNT on mild steel samples in 1M HCl

the investigated BNT is an efficient defender against mild steel corrosion in an acidic medium.

Temperature study

Figure 5 reveals the inhibition efficiencies with various concentration of BNT in 1M HCl solution at different temperatures ranging from 305K to 335 K. It can be seen that moderate increase in hindered efficiencies from Fig. 5 for all the working concentrations (30, 50 and 100 ppm) and the inhibition efficiencies for lower concentration (10 ppm) falls in all studied temperatures. It suggests that the decreasing efficiency at elevated temperature is attributed to physical adsorption while the increasing efficiencies are associated with chemisorptions or both physical and chemical interactions[24]. The values of corrosion rates and the inhibition efficiencies are summarized in Table 3 and the inhibition efficiencies increase with increasing BNT concentration and the maximum efficiency obtained is 93.26%. The temperature study suggests that the adsorption process of BNT on mild steels favors at elevated temperatures in the 1M HCl atmosphere.

Thermodynamic activation parameters

The activation energy (Ea) and pre-exponential factor (A) were acquired by the following Arrhenius equation 7

$$\log CR = \log A - \frac{Ea}{RT} \qquad \ldots(7)$$

Where, R is the universal gas constant, CR is the corrosion rate ($mg.cm^{-2}.h^{-1}$) and T is the temperature (K).

Figure 6 represents the straight lines of Arrhenius plots that are attained by plotting to log CR Vs 1000/T with slope (Ea/R) and intercept (log A). Also, Ea and A values are determined from the slope and intercept respectively and listed in Table 4 As we see in Table 4, the decreasing values of activation energy as rising inhibitor concentration which stand for chemical adsorption[25]. Moreover, we observe the decreasing values of the Arrhenius factor support the corrosion process is effectively prohibited by the adsorption of BNT onto the metal surface.

In the same way, the thermodynamic activation parameters such as entropy of activation (ΔS*) and

Table 3 — Effect of temperature on the inhibition efficiencies for different concentrations of BNT on mild steel specimens in 1M HCl

Conc.(ppm)	CR ($mg.cm^2.h^{-1}$)				I.E (%)			
	305 K	315K	325K	335K	305K	315K	325K	335K
Blank	704.70	1149.83	1636.80	2138.33	-	-	-	-
10	466.28	870.15	1314.98	1886.40	33.83	24.32	19.66	11.78
30	147.15	223.73	271.28	312.60	79.12	80.54	83.43	85.38
50	100.13	115.28	136.05	162.23	85.79	89.97	91.69	92.41
100	60.98	98.40	118.58	144.08	91.35	91.44	92.76	93.26

Table 4 — Thermodynamic activation parameters for BNT on mild steel specimens in 1M HCl

Conc.(ppm)	E_a ($KJ.mol^{-1}$)	A ($g.cm^2.h^{-1}$)	ΔH^* ($KJ.mol^{-1}$)	ΔS^* ($JK^{-1}.mol^{-1}$)	E_a-ΔH^*
Blank	31.38	1.75×10^9	28.74	111.24	2.65
10	39.23	2.59×10^{10}	36.59	135.67	2.64
30	20.98	7.33×10^6	20.98	67.72	2.66
50	23.63	6.15×10^6	18.32	66.26	2.67
100	13.69	2.17×10^5	11.02	38.45	2.65

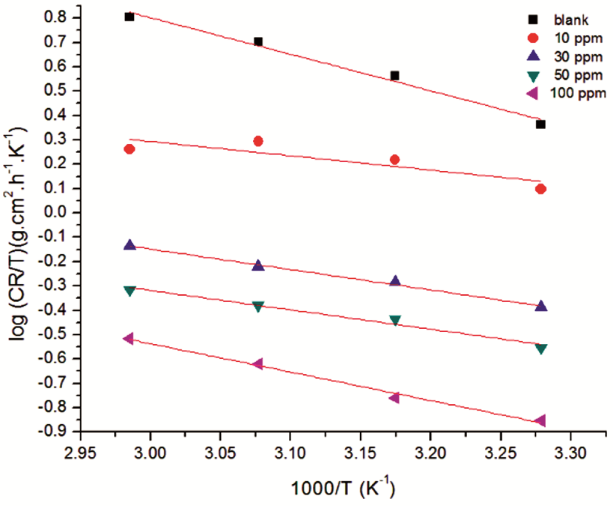

Fig. 6 — Arrhenius plots for various concentrations of BNT on mild steel samples in 1M HCl

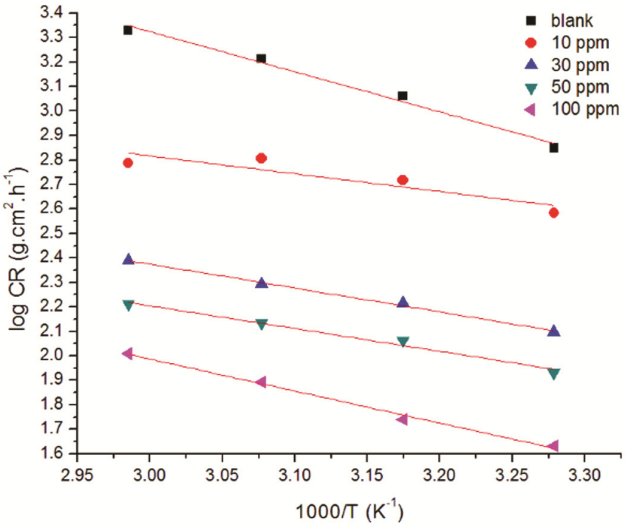

Fig. 7 — Transition state plots for various concentrations of BNT on mild steel samples in 1M HCl

enthalpy of activation (ΔH^*) were determined from the following transition state equation 8

$$\log\left(\frac{CR}{T}\right) = \log\left(\frac{RT}{Nh}\right) + \left(\frac{\Delta S*}{2.303R}\right) \quad \ldots(8)$$

where h is Planck's constant and N is Avogadro's number.

Transition state plots are obtained by plotting log CR/T Vs 1000/T with slope ($-\Delta H^*/2.303R$) and intercept [(log (R/Nh) + $\Delta S^*/2.303R$] of the straight lines as shown in Fig. 7. The values of ΔH^* and ΔS^* are calculated from the slope and intercept respectively and the values for enthalpy of activation and entropy of activation are presented in Table 4.

It reveals the positive values of ΔH^* indicating the adsorption process is endothermic and characteristic chemisorptions[26]. The negative values of ΔS^* suggesting the entropy decreases at metal solution interface due to the displacement of water molecules adsorbed on the metal surface by BNT species[27]. Further, Table 4 shows the difference between the values of Ea and ΔH^* for all the concentrations are approximately equal to 2.61 $KJ.mol^{-1}$ (average value of RT) which gratify the equation Ea - ΔH^* = RT and it mention that the corrosion process is controlled by the thermodynamic activation parameters[28]. Hence, the effect of temperature on the adsorption process clearly explains the adsorption mechanism involving through chemical interactions.

Langmuir adsorption isotherm

The mechanism of the corrosion inhibition process was described by many isotherm models and this adsorption process follows Langmuir isotherm. The Langmuir isotherm parameters were achieved by the following equation 9

$$\frac{C_{inh}}{\theta} = \frac{1}{K_{ads}} + C_{inh} \quad \ldots(9)$$

where C_{inh} is the concentration of BNT (ppm), θ is the Surface coverage and K_{ads} is the equilibrium adsorption constant of the adsorption process.

The equilibrium constant values (K_{ads}) are obtained from the intercept of the straight lines by plotting C_{inh}/θ Vs C_{inh} for various concentrations of BNT at different temperatures are shown in Fig. 8 and recorded in Table 5. From the tabulated results, the increasing values K_{ads} at raised temperatures suggesting the strong adsorption and we can also perceive the linear regression coefficient (R^2) values are closed to 1 which indicates the adsorption process follows Langmuir isotherm. The adsorption standard free energy values (ΔG^0_{ads}) were determined using the following equation 10

$$\Delta G_{ads} = \left[-RT\ In(55.5K_{ads})\right] \quad \ldots(10)$$

where R is gas constant, T is the thermodynamic temperature (K), 55.5 is the concentration of water in tested solutions and K_{ads} is the adsorption equilibrium constant.

It can be seen from Table 5 that the ΔG^0_{ads} values ranged from -33.25 to 36.61 KJ.mol^{-1}which expose that the adsorption process involving both physical and chemical adsorptions[29].

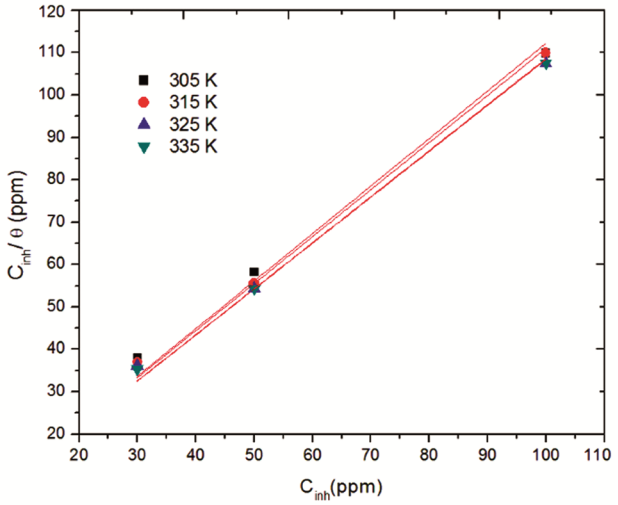

Fig. 8 — Langmuir isotherm for BNT on mild steel specimens in 1M HCl at different temperatures

Table 5 — Langmuir parameters for BNT on mild steel specimens in 1M HCl at different temperatures

Temp (K)	Langmuir isotherm		
	K_{ads} (L.mol^{-1})	ΔG^0_{ads} (KJ.mol^{-1})	R^2
305	8912.42	-33.25	0.9975
315	9006.66	-34.37	0.9986
325	9206.83	-35.52	0.9987
335	9222.97	-36.61	0.9992

Surface interpretation

SEM

Figure 9a-9c displays the SEM examination of bare steel, unprotected surface and protected surface in 1M HCl solution. The polished steel before immersion exhibits the smooth surface as shown in Fig. 9a and the mild steel after immersion in 1M HCl solution exposes severe damages as shown in Fig. 9b. Further, Fig. 9c reflects the steel surface without cracks and pits in the presence of BNT in 1M HCl solution which corroborates the thin film formation on the metallic surface against mild steel corrosion by the adsorption of BNT species in the corrosive medium[30].

EDS

The electron dispersive spectra of mild steel specimens before immersion, after immersion and in the presence of BNT respectively were plotted. It displays the characteristic peaks of Fe, C and O present in the bare steel and reflects the existence of chlorine peak due to rust formation. Besides that, it also shows the nitrogen peak along with the inspected elements which indicates that the corrosion damages are reduced by the adsorption of BNT molecule on the mild steel surface. The EDS data of the examined steel specimens are registered in Table.6 and the weight percentage values support that the corrosion behavior is hindered by the development of protective film via nitrogen coordination with the steel surface in 1M HCl solution[31].

AFM

Inspection of Table 7 shows that the average roughness values for polished mild steel, specimens in the absence and presence of BNT are 160.65nm, 895.36 nm and 212.72 while the corresponding RMS values are 195.31nm, 1500.1nm and 262.45 nm respectively. The larges values of roughness noted for

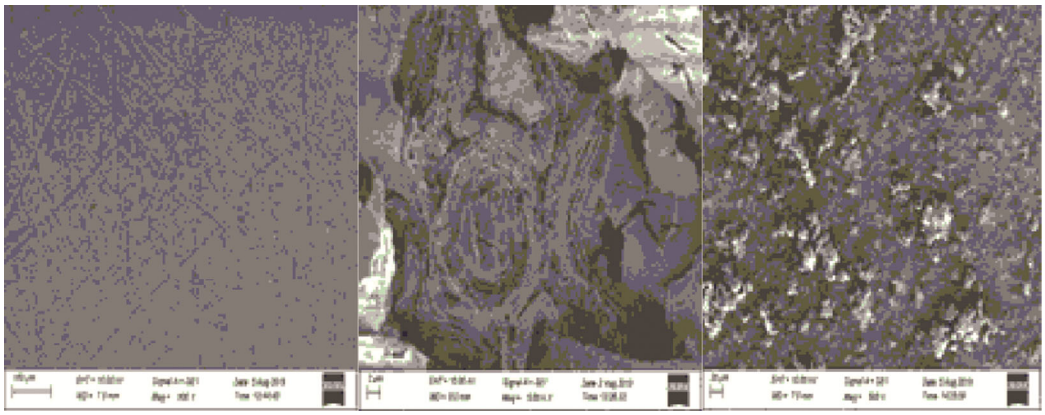

Fig. 9 — SEM images of (a) polished mild steel; (b) unhindered sample and (c) hindered sample with BNT in 1M HCl

Table 6 — Elemental analysis for polished mild steel specimen, unprotected and protected steel specimens in 1M HCl

Specimens	Weight %				
	Fe	O	C	Cl	N
Polished mild steel	79.82	7.98	12.20	-	-
Unprotected mild steel	49.66	43.44	5.84	1.06	-
Protected mild steel with BNT	75.67	9.73	13.21	-	1.39

Table 7 — AFM parameters for bare steel, unprotected and protected steel specimens in 1M HCl

Samples	Average Roughness (R_a)nm	RMS roughness (R_q) nm
Bare steel surface	160.65	195.31
Unprotected surface	895.36	1500.1
Protected surface with BNT inhibitor	212.72	262.45

unprotected surfaces indicating the metal surface is severely damaged by the corrosive medium. In the presence of inhibitor, the roughness values are closer to the bare steel which corroborates that the corrosion attacks are reduced by the adsorption of inhibitor.

It is also evident that the bare steel shows the smoother surface and the unprotected specimen reveals rough surface due to acid attack Further, it exhibits the roughness of the steel surface is considerably reduced by the adsorption BNT in 1M HCl solution[32].

Mechanism of corrosion inhibition

The electrochemical corrosion reactions are hindered by the adsorption of BNT on to the metal surface either by physical adsorption, chemical adsorption, or both. In this study, all the verdicts explained that the inhibition process is carried out through both the physical and chemical interactions[33,34]. Protonation happens at the heteroatom of BNT while chloride ions adsorb on the metal surface exposed in 1M HCl solution and the surface become negatively charged. Thus, the electrostatic interaction takes place between the cationic BNT species and anionic metal surface.

Also, chemical interaction takes place in two ways; (i) the interaction between the unshared pairs of the nitrogen atom of BNT and the vacant d orbital of the Fe atoms. (ii) π electrons of the aromatic rings present in BNT molecule interact with the d orbital of the Fe atoms resulting in chemisorptions. Both kinds of mechanisms are expressed in the following equations11 &12

$$(FeCl^-)_{ads} + BNT^+ \rightarrow [(FeCl^-)(BNT^+)]_{ads} \quad \ldots(11)$$

$$Fe^{2+} + BNT_{(ads)} \rightarrow [Fe\text{-}BNT]^{2+}_{(ads)} \quad \ldots(12)$$

Moreover, the thermodynamic activation parameters suggested that the adsorption process is carried out by the displacement of water molecules [35] on the mild steel surface by BNT and is given by the following equation 13

$$BNT_{(sol)} + nH_2O_{(ads)} \rightarrow BNT_{(ads)} + nH_2O_{(sol)} \quad \ldots(13)$$

where n is the number of water molecules replaced by BNT molecules.

Thus, all the data proposed that the corrosion process is effectively controlled by both the physical and chemical adsorption but chemical adsorption is more predominant than the electrostatic attraction.

Conclusion

The anti-corrosive effect of BNT molecule on mild steel corrosion in 1M HCl solution was investigated by mass loss, polarization and impedance techniques. All the explored methods revealed that they were in

good agreement with each other and BNT act as a mixed type inhibitor with cathodic predominance according to polarization study. The thermodynamic activation parameters suggested that the adsorption process is endothermic, spontaneous and decreased the solution entropy. The adsorption process obeyed Langmuir isotherm and the mechanism involved both the physical and chemical interactions but more chemisorptions were reported. Moreover, SEM, EDS and AFM analysis corroborated the corrosion rate is hindered by the development of protective coating on the mild steel. Therefore, all the conclusions corroborated that BNT was a proficient inhibitor on mild steel surface in the 1M HCl solution.

Acknowledgement

The authors are highly thankful to PG and Research Department of Chemistry, Rajah Serfoji Government College (Autonomous), Thanjavur-613005 for providing laboratory facilities.

References

1 Eddy NO & Ita BI, *J Mol Model*, 17 (2011) 359.
2 Strickland D M, *Ind Eng Chem*, 15 (1923) 566.
3 Goulart C M, Esteves-Souza A, Martinez-Huitle C A, Rodrigues C J F, Maciel M A M & Echevarria A, *Corros Sci*, 67 (2013) 28.
4 Zarrok H, Saddik R, Oudda H, Hammouti B, El Midaoui A , Zarrouk A, Benchat N & Ebn Touhami M, *Der Pharm Chem*, 4 (2011) 272.
5 Al Hamzi A H, Zarrok H, Zarrouk A, Salghi R, Hammouti B, Al-Deyab S S, Bouachrine M, Amine A & Guenoun F, *Int J Electrochem Sci*, 8 (2013) 2586.
6 Zarrouk A, Hammouti B, Zarrok H, Salghi R, Dafali A, Bazzi Lh, Bammou L & Al-Deyab S S, *Der Pharm Chem*, 4 (2012) 337.
7 Abd El Rehim S S, Sayyah S M, El-Deeb M M, Kamal S M & Azooz R E, *Int J Ind Chem*, 7 (2016) 39.
8 Sudhish K S, Eno E E, *Int J Electrochem Sci*, 6 (2011) 3277.
9 Singh A K & Quraishi M A, *Int J Electrochem Sci*, 7 (2012) 3222.
10 Oyebamiji A K & Adeleke B B, *Int J Corros Scale Inhib*, 7 (2018) 498.
11 Jeeva P A, Mali G S, Dinakaran R, Mohanam K & Karthikeyan S, *Int J Corros Scale Inhib*, 8 (2019) 1.
12 Al-Amiery A A, Kadhum A A H, Kadihum A, Mohamad A B, Chong K, How C K & Junaedi S, *Mater*, 7 (2014) 787.
13 Rahmani H, Ismaily Alaoui K, Emran K M, El Hallaoui A, Taleb M, El Hajji S, Labriti B, Ech-chihbi E, Hammouti B & El-Hajjaji F*, Int J Electrochem Sci*, 14 (2019) 985.
14 Fernandes C M, Alvarez L X, Dos Santos N E, Maldonado Barrios A C & Ponzio A E, *Corros Sci*, 149 (2019) 185.
15 Desai P S & Indorwala N S, *Res J Chem Sci*, 5 (2015) 30.
16 Scendo M & Staszewska-Samson K, *Int J Electrochem Sci*, 12 (2017) 5668.
17 Kozaderov O A, Shikhaliev Kh S, Prabhakar Ch, Shevtsov D S, Kruzhilin A A, Komarova E S, Potapov A Yu & Zartsyn I D, *Int J Corros Scale Inhib*, 8 (2019) 422.
18 Gonzalez-Olvera R, Espinoza-Vazquez A, Negron-Silva G E, Palomar-Pardave M E, Romero-Romo M A & Santillan R, *Molecules*,18 (2013) 15064.
19 Verma D K, Ebenso E E, Quraishi M A & Verma C, *Results in Physics*, 13 (2019) 102194.
20 Paulraj J, Gangaprasad D, Vajjiravel M, Karthikeyan K & Elangovan J, *J Chem Sci*, 130 (2018) 44.
21 Oboz I B & Obi-Egbedi N O, *Corros Sci*, 52 (2010) 198.
22 Ashassi-Sorkhabi H, Majidi M R & Seyyedi K, *Appl Surf Sci*, 225 (2004) 176.
23 Abdel-Aal M S & Morad M S, *British J Corros*, 36 (2001) 253.
24 Nataraja S E, Venkatesha T V, Manjunatha K, Boja Poojary, Pavithra M K & Tandon H C, *Corros Sci*, 53 (2011) 2651.
25 Al-Sabagh A M, Kandil N Gh, Ramadan O, Amer N M, Mansour R & Khamis E A, *Egypt J Petrol*, 20 (2011) 47.
26 Liao L L, Mo S, Lei Lei J, Qun Luo H & Bing Li N, *J Colloid Interface Sci*, 474 (2016) 68.
27 Yadav D K, Quraishi M A & Maiti B, *Corros Sci*, 55 (2012) 254.
28 Ostovari A H, Hoseinieh S M, Peikari M, Shadizadeh S R & Hashemi S J, *Corros Sci*, 51 (2009) 1935.
29 Hazazi O A, Fawzy A & Awad M, *Int J Electrochem Sci*, 9 (2014) 4086.
30 Tan B, Zhang S, Qiang Y, Guo L, Feng L & Liao C, *J Colloid Interface Sci*, 526 (2018) 268.
31 Van Ooij W J, *Surf Technol*, 6 (1977) 1.
32 Shanmughan S K, Kakkassery J T, Raphael V P & Kuriakose N, *Current Chem Lett*, 4 (2015) 67.
33 Bentiss F, Traisnel M & Lagrenee M, *Corros Sci*, 42 (2000) 127.
34 Benali O, Larabi L, Tabti B & Harek Y, *Anti Corros Methods Mater*, 52 (2005) 280.
35 Li L, Zhang X, Lei J, He J , Zhang S & Pan F, *Corros Sci*, 63 (2012) 82.